LABORATORY EVALUATION OF SAND UNDERDRAINS

By Te-Fu Chiu[1] and Charles D. Shackelford,[2] Member, ASCE

ABSTRACT: Constant-head hydraulic conductivity tests are performed on layered heterogeneous porous media to evaluate the use of underdrains to calculate the hydraulic conductivity of an overlying, less permeable medium. The layered profiles consist of a barrier layer comprising sand mixed with 10% kaolin, overlying a foundation layer comprising sand mixed with only 5% kaolin. Underdrains are evaluated by replacing excavated portions of the foundation layer with only sand. The results indicate that preferential flow of water occurs around, rather than through, the sand underdrains resulting in an underestimate of the measured hydraulic conductivity of the barrier layer assuming 1D, saturated flow in accordance with standard practice. The observed preferential flow effect is consistent with previously published numerical simulations of unsaturated flow through similarly layered heterogeneous soil profiles that indicate lateral flow around underdrains due to the contrast in unsaturated properties of the soils. The results of this study have important ramifications with respect to the use of underdrains to measure in situ hydraulic conductivity of compacted clay liners for waste containment.

BACKGROUND

Underdrains, also known as collection lysimeters or pan lysimeters, typically are constructed beneath compacted clay liners used in waste disposal facilities. The construction procedure typically involves (1) excavating a trench into the foundation soil; (2) lining the trench with a relatively impervious material (e.g., a geomembrane); (3) backfilling the lined trench with a highly permeable drainage material (e.g., sand, gravel, geocomposite); (4) saturating the drainage material with water to check for leaks; (5) draining the saturated drainage material; and (6) covering the drainage material with a filter fabric. Underdrains initially were perceived as early detection monitoring systems used to detect leaks in or failure of the liner system. However, underdrains also have been used to measure in situ hydraulic conductivity of clay liners (Daniel 1989; Sai and Anderson 1990).

Several case histories involving the use of underdrains to measure in situ hydraulic conductivity of clay liners are summarized in Table 1. Three observations are readily apparent from the data presented in Table 1. First, the elapsed times for the reported field-measured hydraulic conductivity values are all $\leq$8 years. Second, the field-measured hydraulic conductivity values in six of the seven cases decrease with time. Third, the two underdrains for the Marathon County Landfill eventually were considered dry after 4 and 8 years of service, and the underdrain below the Keele Valley Landfill apparently experienced no measurable flow after 6 years of service.

The observations from the data in Table 1 may be attributed to several factors. For example, the initially relatively high hydraulic conductivity values could be due to initial drainage of water from the initially saturated underdrain and/or production of consolidation water from the clay liner as suggested by Bonaparte and Gross (1990). The decrease in hydraulic conductivity with time also may be due to consolidation of the clay liner upon waste loading, and the eventual dry or no flow conditions of the underdrains may be due to clogging of the filter or drainage material.

The decreases in hydraulic conductivity with time apparent in the field-measured hydraulic conductivities reported in Table 1 also are consistent with expected behavior based on 2D numerical simulations of unsaturated flow through layered heterogeneous soil illustrated schematically in Fig. 1 as presented by Chiu and Shackelford (1994), Shackelford et al. (1994), and Shackelford and Chiu (1997). Based on the results of their simulations, lateral flow around the underdrain occurs as a result of the differences in soil-water characteristics [Fig. 1(b)] and unsaturated hydraulic conductivity-suction relationships [Fig. 1(c)] among the clay liner, foundation soil, and underdrain. The contrast in unsaturated soil properties due to the placement of a relatively fine soil over a relatively coarse soil results in the ''capillary barrier effect'' that recently has been proposed for the design of alternative cover systems [e.g., Sailie (1985), Morel-Seytoux (1993), Benson and Khire (1995), Morris and Stormont (1997), and Khire et al. (1999)]. The preference for lateral flow of water through the finer textured soil along the interface between the finer textured soil and the coarser textured soil also has been referred to as the ''wicking effect'' (Yeh et al. 1994).

Daniel (1989) recognized the potential for lateral flow around underdrains by stating that the tendency for flow to be other than 1D may be minimized by making the width of the pan (underdrain) greater than the thickness of the liner (i.e., $W > D$). Cartwright and Krapac (1990) noted that the soil-gravel interface of underdrains acts as a barrier to unsaturated flow resulting in inaccurate estimates of breakthrough time and measured flux through the liner due to lateral flow around the lysimeter to the native (foundation) soil. As a result, Cartwright and Krapac (1990) questioned the practicality of putting lysimeters (underdrains) under a liner to monitor leakage through the liner.

Chiu and Shackelford (1994) numerically evaluated the effects of the ''underdrain size ratio,'' W/D, and the initial saturation of the clay liner on the potential for lateral unsaturated flow around underdrains. They found that a low W/D increased the percentage of flow around the underdrain, but no significant influence was indicated for $W/D \geq 5$. Chiu and Shackelford (1994) also found that a lower initial degree of saturation in the clay liner tended to delay the time required to reach steady-state flow conditions but did not appreciably affect the steady-state flux. These observations are consistent with the potential for lateral flow around the underdrain as noted by Daniel (1989) and Cartwright and Krapac (1990). However, no experiments were conducted by Chiu and Shackelford (1994) to verify their conclusions.

Bews et al. (1997, 1999) recently evaluated the design of collection lysimeters placed directly in waste rock to monitor the performance of covers at mine waste sites in semiarid climates. Their evaluations included numerical simulations and some measured fluxes based on laboratory prototype column

[1]Engr., Sinotech Engineering Consultants, Ltd., 171 Nanking E. Rd., Sect. 5, Taipei, Taiwan.

[2]Prof., Dept. of Civ. Engrg., Colorado State Univ., Fort Collins, CO 80523 (corresponding author). E-mail: shackel@engr.colostate.edu

Note. Discussion open until April 1, 2001. To extend the closing date one month, a written request must be filed with the ASCE Manager of Journals. The manuscript for this paper was submitted for review and possible publication on July 23, 1998. This paper is part of the ***Journal of Geotechnical and Geoenvironmental Engineering***, Vol. 126, No. 11, November, 2000. ©ASCE, ISSN 1090-0241/00/0011-0990–1001/$8.00 + $.50 per page. Paper No. 18864.

TABLE 1. Case Histories Involving Use of Underdrains to Measure Hydraulic Conductivity [Modified after Chiu (1995)]

Landfill (1)	Clay liner thickness, D (m) (2)	Size of underdrain (3)	Field hydraulic conductivity (m/s) and date of measurement (4)	Elapsed time (years) (5)	Field hydraulic conductivity/ laboratory hydraulic conductivity (6)	Reference (7)
Nekoosa Papers	1.2	0.38 × 6.10 m	1×10^{-9} (1981)–4×10^{-9} (1983)	3	NA	Kmet and Lindorff (1983)
Marathon County	1.2	5.5 × 12.2 × 0.91 m	2×10^{-10} (12/80)–Dry (12/81)	8	6.7–0	Kmet and Lindorff (1983);
		3.7 × 30.5 × 0.91 m	5×10^{-11} (9/85)–Dry (12/86)	4	1.6–0	Gordon et al. (1989)
Portage County	1.5	688 m^2	9×10^{-11} (7/84)–1×10^{-11} (12/87)	3	0.9–0.1	Gordon et al. (1989)
Sauk County	1.5	83.6 m^2	4×10^{-10} (9/83)–1×10^{-10} (12/87)	4	0.5–0.125	Gordon et al. (1989)
Keele Valley	0.3–0.5	15 × 15 m (within liner)	1×10^{-9} (3/84)–1×10^{-11} (3/88)	4	0.1–0.33	Reades et al. (1987, 1990)
	1.2	15 × 15 m (below liner)	No flow (5/90)	6	0	

Note: NA = not available.

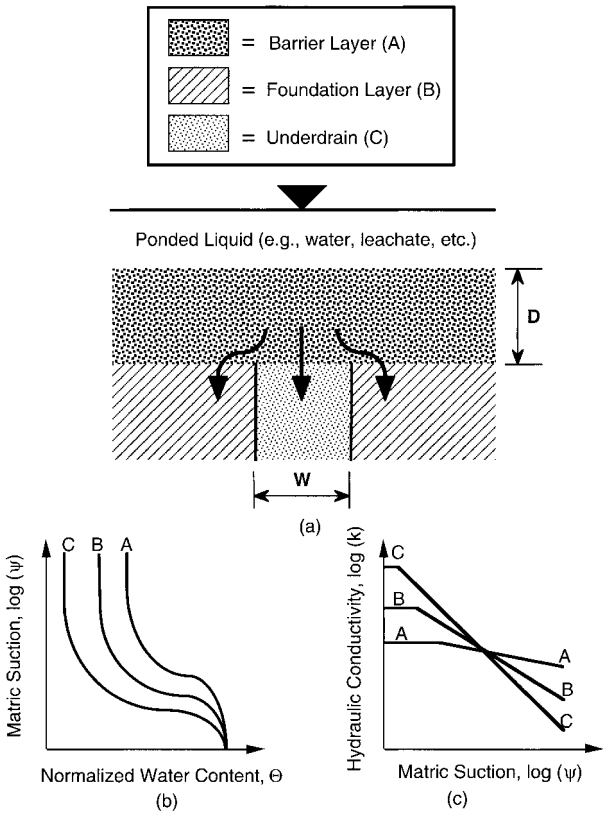

FIG. 1. Schematic Illustration of Hypothetical Existence of Lateral Flow around Underdrain in Waste Containment Scenario: (a) Profile; (b) Soil-Water Characteristics; (c) Hydraulic Conductivity-Suction Relationships [after Chiu and Shackelford (1994) and Shackelford and Chiu (1997)]

tests. Unlike the scenario depicted in Fig. 1, the upper boundary condition in their studies was flux controlled in accordance with typical conditions associated with covers, and the resulting fluxes were relatively low, typically less than the saturated hydraulic conductivity of the waste rock. Nonetheless, their results show that lateral flow around collection lysimeters occurs in the case where the backfill material in the collection lysimeter is coarser than the surrounding material (e.g., waste rock), and the infiltrating fluxes are low. Bews et al. (1997, 1999) noted that such observed behavior is consistent with unsaturated flow theory and the unsaturated properties of the waste rock and the backfill material used for the collection lysimeter.

Although there appears to be some awareness of the potential for preferential flow around underdrains due to the existence of unsaturated flow conditions, experimental studies documenting this effect for the scenario depicted in Fig. 1 are either lacking or nonexistent in the published literature. Also, the apparent, widespread use of underdrains as documented in Table 1 suggests that a general awareness of this potential effect, particularly in the practicing engineering community, is lacking. Thus, the primary objective of this study is to evaluate experimentally the potential existence and resulting effect, if any, of lateral flow around underdrains in layered heterogeneous porous media.

MATERIALS AND METHODS

Soils and Soil Mixtures

Since the potential for unsaturated flow around underdrains apparently exists because of a contrast in unsaturated soil properties, as illustrated schematically in Fig. 1, the primary consideration for the testing program was to use a soil layering scenario that resulted in a finer textured soil overlying two coarser textured soils, one of which was an underdrain. In general, the lateral flow effect becomes increasingly more pronounced as the contrast in the properties of the finer and coarser soils increases. However, the contrast in soil properties does not have to be great to result in the effect. For example, sand and silty sand have been used as the overlying (barrier) layer with a gravel and a sand, respectively, as the underlying layer in several capillary barrier covers [e.g., Benson and Khire (1995)]. Thus, the objective in choosing the porous media to be tested was to establish a sufficient contrast in the properties of the porous media to cause the expected lateral flow effect, without exaggerating the contrast to the extent that prolonged test durations would have been required.

TABLE 2. Physical Properties of Sand and Kaolin Used in This Study

Property (1)	ASTM standard (2)	Value	
		Sand[a] (3)	Kaolin[b] (4)
Water content, w (%)	D 4959	0	0.4
Specific gravity, G_s	D 854	2.65	2.62
Liquid limit, LL (%)	D 4318	NA	56
Plastic limit, PL (%)	D 4318	NA	33
Plasticity index, PI (%)	D 4318	NA	23
Sand (0.074–4.75 mm) (%)	D 421	100	0
Silt (0.002–0.074 mm) (%)	D 422	0	60
Clay (<0.002 mm) (%)	D 422	0	40
USCS Classification	D 2487	SP	MH

Note: USCS = Unified Soil Classification System; NA = not available.
[a]Sand is 16–40 Silica Sand from Colorado Lien Co., Fort Collins, CO.
[b]Kaolin is Standard Air Float from Georgia Kaolin Co., Union, N.J.

TABLE 3. Physical Properties of Component Materials Used in This Study

Property (1)	ASTM standard (2)	Value: Barrier soil mixture (3)	Value: Foundation soil mixture (4)	Value: Underdrain sand (5)
Sand content (%)	NA	90	95	100
Kaolin content (%)	NA	10	5	0
Sand (0.074–4.75 mm) (%)	D 421	90	95	100
Silt (0.002–0.074 mm) (%)	D 422	6	3	0
Clay (<0.002 mm) (%)	D 422	4	2	0
Classification (USCS)	D 2487	SP-SC	SP	SP
Maximum dry unit weight $\gamma_{d\,max}$ (kN/m^3)[a]	D 698	17.2	16.5	—
Optimum gravimetric water content, w_{opt} (%)	D 698	14.0	13.5	—
Optimum volumetric water content, θ_{opt}	NA	0.246	0.227	—
Saturation at θ_{opt}, S_{opt} (%)	NA	73.7	61.9	—
Residual volumetric water content, θ_r[b]	NA	0.0609	0.0454	0.0284
Saturated volumetric water content, θ_s	NA	0.334	0.367	0.435
Maximum volumetric water content, θ_m[c]	NA	0.282	0.321	0.387
Saturation at θ_m, S_m (%)	NA	84.4	87.5	89.0
Steady-state hydraulic conductivity, k_{DRP} (m/s)[c]	NA	1.3×10^{-7}	7.0×10^{-7}	5.0×10^{-5}

Note: USCS = Unified Soil Classification System; NA = not available.
[a]1 kN/m^3 = 6.365 lb/ft^3.
[b]Based on analyses of soil-water characteristic data by Chiu and Shackelford (1998).
[c]Based on results of double-ring permeability tests from Chiu and Shackelford (1998).

Based on this objective, a sand was chosen for use as the underdrain material, and mixtures of the sand with 5 and 10% of a processed kaolin clay were chosen for use as the foundation layer and the barrier layer, respectively. The mixtures of the sand and kaolin were chosen to improve the ability to control the properties of the different porous media. The processed clay was chosen to ensure relative homogeneity of the clay portion of the sand-clay mixtures, and kaolin was chosen as the processed clay to minimize any secondary effects, particularly shrinkage and swelling, that typically are associated with more active processed clay soils, such as sodium bentonite. The 5 and 10% kaolin contents proved to be sufficiently high to provide the necessary contrast in soil properties, yet sufficiently low to prevent excessive test durations. The physical properties of the sand and kaolin used as soil constituents for the soil mixtures are given in Table 2, whereas the relevant physical properties of component materials used in the study are presented in Table 3.

The hydraulic conductivities (k_{DRP}) shown in Table 3 for the underdrain sand and the two sand-kaolin mixtures are based on the results of double-ring hydraulic conductivity tests that indicated essentially no sidewall leakage as reported by Chiu and Shackelford (1998). Although the specimens in these tests were not saturated at steady-state flow, Chiu and Shackelford (1998) noted that the measured k_{DRP} values probably are representative of the maximum hydraulic conductivities that are attainable using rigid-wall permeameters without back-pressure saturation. Also, the k_{DRP} values were essentially identical to hydraulic conductivities that were measured independently in single-ring, plexiglass test cells. Thus, the ability to compact reproducible specimens of the same soil mixtures also was considered to be excellent, an important consideration in the context of the use of these same soil mixtures in this study (Chiu and Shackelford 1998).

Although all of the porous media in Table 3 are classified as coarse-grained materials, a significant contrast in the measured hydraulic conductivities, k_{DRP}, still exists. For example, k_{DRP} of the foundation soil mixture is ~5.4 times higher than k_{DRP} of the barrier soil mixture, and k_{DRP} of the underdrain soil is ~71 times higher than k_{DRP} of the foundation soil mixture. Therefore, k_{DRP} of the underdrain sand is ~380 times higher than k_{DRP} of the barrier soil mixture.

The measured soil-water characteristics and unsaturated hydraulic conductivity versus suction relationships for the underdrain sand and the two sand-kaolin mixtures as reported by Chiu and Shackelford (1998) are shown in Fig. 2. The normalized volumetric water content, Θ, in Fig. 2(a) is defined as follows:

$$\Theta = \frac{\theta - \theta_r}{\theta_m - \theta_r} \tag{1}$$

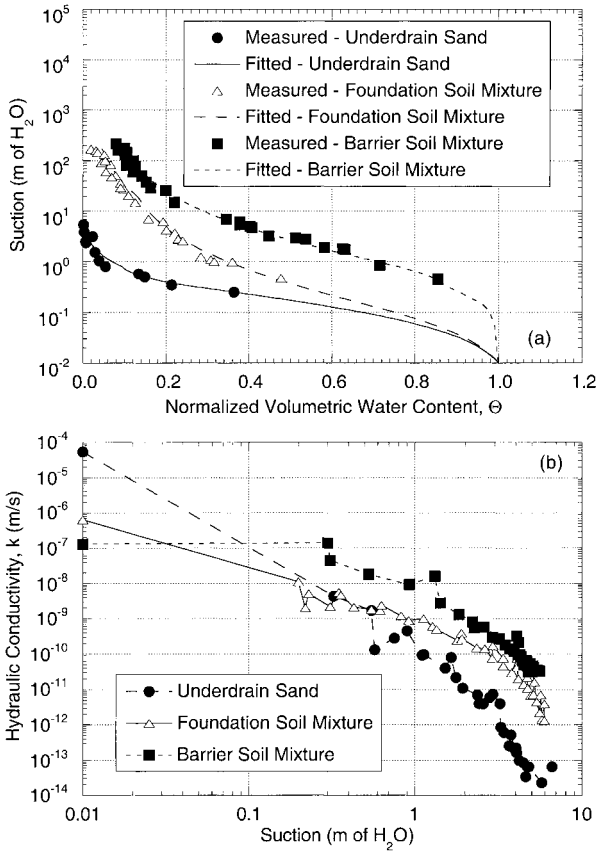

FIG. 2. Measured Unsaturated Properties for Sand and Sand-Kaolin Mixtures Used in This Study: (a) Measured and Fitted (van Genuchten 1980) Soil-Water Characteristics Based on Wetting Process; (b) Hydraulic Conductivity-Suction Relationships Using Instantaneous Profile Method [All Data from Chiu and Shackelford (1998)]

where θ = actual volumetric water content; θ_r = residual volumetric water content; and θ_m = maximum volumetric water content. Values of θ_r and θ_m for the sand and sand-kaolin mixtures are given in Table 3. The maximum volumetric water content, θ_m, is used instead of the saturated volumetric water content, θ_s, in (1) because Chiu and Shackelford (1998) found that θ_m was less than θ_s for the sand and sand-kaolin mixtures due to the existence of entrapped air under wetting conditions.

As expected, the same relative relationships among the soil-water characteristics and unsaturated hydraulic conductivities for the clay liner, foundation soil, and underdrain shown in Fig. 1 are apparent among the soil-water characteristics and unsaturated hydraulic conductivities for the barrier soil mixture (90% sand + 10% kaolin), foundation soil mixture (95% sand + 5% kaolin), and underdrain sand (100% sand) shown in Fig. 2. Thus, the contrast in unsaturated properties required for the desired effect on the basis of the previously reported numerical simulations is evident with respect to the sand and sand-kaolin mixtures used in this study.

Testing Apparatus and Preparation

The testing apparatus, illustrated schematically in Fig. 3, essentially consists of two boxes, constructed with 2.54-cm-thick clear plexiglass plate, that are connected and clamped together between 2.54-cm-thick clear plexiglass plates on the top and bottom to form a single permeability cell. The length by width (plan area) dimensions of the boxes are either 43.5 × 10.2 cm or 106 × 10.2 cm. These exaggerated length-to-width dimensions were desired to promote 2D flow. The height of the lower box, which contains the foundation soil mixture and the sand underdrain, is 5.08 cm, whereas the height of the upper box, which contains the barrier soil mixture and the head space for ponding water, is 12.7 cm.

Two 1.27-cm holes near the top of the upper box were used to supply water continuously to the head-space reservoir

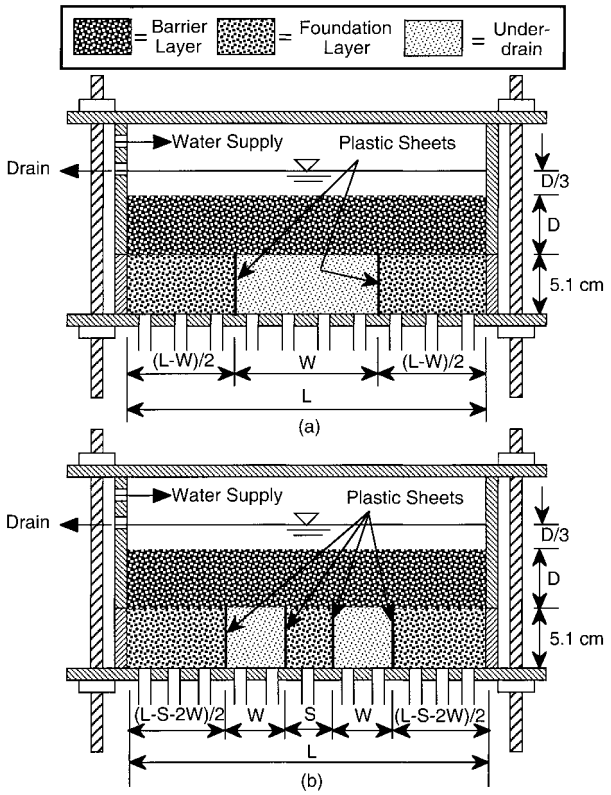

FIG. 3. Schematic Cross Sections of Testing Cells: (a) Single Underdrain Configuration; (b) Double Underdrain Configuration (Not to Scale)

through a hose attached to a faucet and to maintain a constant height of ponded water through drainage during the test. A series of 0.32-cm drainage holes with center-to-center spacings of 2.54-cm also was bored along the centerline of the bottom plate beneath the plan area of the lower box to collect the outflow from each region of the cell.

Preparation and placement of the foundation and barrier soil mixtures involved mixing the sand with the appropriate amount of kaolin at optimum water content for the mixture (Table 3) using deaired tap water, curing the wetted sand-kaolin mixture in double zip-lock bags for 24 h, and compacting the mixture into the testing cell using a tamping rod. The amount of the wetted sand-kaolin mixture to be compacted into the testing cell was determined using the maximum dry unit weight for the mixture (Table 3) and the required volume of the mixture in the testing cell.

The foundation soil mixture was placed and compacted into the lower box until the mixture filled the entire box. A sufficient amount of foundation soil mixture was added to the cell such that only one lift of the mixture was needed, thereby preventing the potential effect of lateral flow along interlift zones. After compaction of the foundation soil mixture, but before assembling the two boxes, a specified width of the foundation soil mixture, W, was excavated and replaced with the sand to form the underdrain, as illustrated in Fig. 3(a). The width, W, was determined by the desired underdrain size ratio, W/D, representing the ratio of width of the sand underdrain to the thickness (depth) of the barrier soil mixture. In the case of two underdrains, illustrated in Fig. 3(b), the spacing between the underdrains, S, was determined by the desired underdrain spacing ratio, S/W. Before placement of the sand in the excavated space, two 0.32-cm-thick plexiglass plates were inserted against the foundation soil mixture to act as physical barriers to flow between the sand underdrain and the foundation soil mixture, and the gaps between the plates and walls of the box were filled with silicon caulk to form a watertight seal. After placement of the sand used for the underdrain, the sand was densified by percolating water through the sand in the testing cell. If densification of the sand was observed, additional sand was placed on top of the previously densified sand, and water again was percolated through the sand underdrain. This process, which mimics the initial soaking of underdrains in the field, was repeated until further densification of the sand had stopped.

The barrier soil mixture was compacted in one lift directly into the lower portion of the upper box using the same procedure as used for the foundation soil mixture. The thickness of the barrier soil mixture, D, was based on the desired underdrain size ratio, W/D. After the barrier soil mixture was compacted, the lower and upper boxes were assembled with the top and bottom plates. Before placing the lower box with the compacted foundation soil mixture on the bottom plate, filter paper was placed over the bottom plate contact area to facilitate lateral flow to the drainage holes and to prevent the foundation soil mixture and underdrain sand from washing from the cell during the test, the top of the foundation soil mixture was scarified with a pick to promote bonding between the layers of the barrier and foundation soil mixtures, and silicon caulk was placed on all plexiglass contact areas to provide watertight seals. The assembled testing cell was connected and clamped together through four 0.953-cm threaded tie-rods placed in each corner of the top and bottom plates.

The test commenced after assembling and clamping the testing cell by filling the reservoir rapidly with tap water to the desired level to establish the hydraulic gradient for flow. In all cases, the height of ponded water, D_p, was maintained at one-third the thickness of the barrier layer (i.e., $D_p = D/3$). Also, the drains through the bottom plate were exposed to atmo-

TABLE 4. Summary of Testing Program

Testing program data (1)	Initial Condition							
	As-compacted (2)			Air-dried (3)				
Test number	1	2	3	4	5	6	7	8
Number of underdrains	1	1	1	1	1	1	2	2
Specimen dimensions[a]								
W (cm)	7.62	12.7	25.4	7.62	12.7	25.4	12.7	12.7
D (cm)	7.62	5.08	5.08	7.62	5.08	5.08	5.08	5.08
S (cm)	0	0	0	0	0	0	12.7	25.4
L (cm)	38.4	101	101	38.4	101	101	101	101
Underdrain size ratio *W*/*D*	1	2.5	5	1	2.5	5	2.5	2.5
Underdrain spacing ratio *S*/*W*	0	0	0	0	0	0	1	2

[a]See Fig. 3: *W* = width of underdrain; *D* = thickness of barrier layer; *S* = spacing between underdrains; *L* = length of layered profile.

spheric pressure. As a result, the tests performed in this study essentially represent constant-head hydraulic conductivity tests through layered heterogeneous porous media. Tests were continued at least until steady-state flow was achieved resulting in test durations ranging from 14 to 24 days.

Testing Program

The testing program consisted of a total of the eight tests outlined in Table 4. The dimensions of the various segments in the test cells with respect to Fig. 3 also are given in Table 4. The first three tests (Test Nos. 1–3) were performed to evaluate the effect of the layered profile tested immediately after compaction, whereas the last five tests were performed to evaluate the potential effect of air drying the compacted sand-kaolin mixtures prior to assembling the cell (Test Nos. 4–6) and the effect of using more than one underdrain (Test Nos. 7 and 8). The sand-kaolin mixtures and underdrain sand in Test Nos. 4–8 were air dried simply by exposure to the ambient atmosphere under controlled (enclosed) laboratory conditions for 24 h prior to assembling the testing apparatus and commencing the tests.

In measuring the soil-water characteristics and unsaturated hydraulic conductivities for the same sand-kaolin mixtures, Chiu and Shackelford (1998) reported that air drying the sand-kaolin mixtures was effective in decreasing the volumetric moisture content of the mixtures from the as-compacted value, θ_{opt}, to a value nearer the residual water content, θ_r. Air drying the compacted sand-kaolin mixtures increases the initial suction in, and the storage capacity of, the mixtures and, therefore, was expected to affect the contrast in the initial conditions among the three porous media in the cell (e.g., Fig. 2). As previously noted, numerical simulations on similarly layered soil profiles have indicated that a lower initial degree of saturation in the clay liner tends to delay the time required to reach steady-state flow conditions, but does not appreciably affect the steady-state flux (Chiu and Shackelford 1994; Shackelford et al. 1994). Thus, air drying was expected to affect only the time required to achieve steady-state flow conditions, not necessarily the results after steady-state flow had been achieved, provided the sand-kaolin mixtures did not crack. However, cracking of the sand-kaolin mixtures was not expected to be a problem due to (1) the low clay contents of the mixtures; (2) the low activity of kaolin clay; (3) the short duration of drying; and (4) the controlled environment in which the tests were performed. Also, cracking was not evident in the tests performed by Chiu and Shackelford (1998) using the same sand-kaolin mixtures.

Underdrain size ratios, *W*/*D*, of 1, 2.5, and 5 were evaluated in Test Nos. 1, 2, and 3, respectively, for initial conditions corresponding to immediately after compaction, and in Test Nos. 4, 5, and 6, respectively, for initial conditions corresponding to 24 h after air drying the soils. The upper limit on *W*/*D* of 5 was based on previous numerical simulations performed by Chiu and Shackelford (1994) that indicated no significant lateral flow effect for $W/D \geq 5$. The potential effect of lateral flow in the case of two sand underdrains was evaluated by comparing the results from Test No. 5 for *W*/*D* = 2.5 and a underdrain spacing ratio, *S*/*W*, of zero (i.e., only one underdrain) with the results for Test Nos. 7 and 8 with *W*/*D* = 2.5 and *S*/*W* = 1 and *SW* = 2, respectively.

RESULTS

Cumulative Percolation

For the case of a single underdrain, the cumulative volumes of percolation normalized with respect to each of the three outflow areas of the test cell for tests performed immediately after compaction (Test Nos. 1–3) and after air drying (Test Nos. 4–6) are shown in Figs. 4 and 5, respectively. The normalized cumulative percolations for the two tests performed to evaluate the potential effect of lateral flow around two identical sand underdrains separated by a distance *S* (Test Nos. 7 and 8) are plotted versus time in Fig. 6. The results for Test No. 5 with the same *W*/*D* (=2.5) and only one sand underdrain (i.e., *S*/*W* = 0) also are shown in Fig. 6 for comparison.

Several observations are apparent from the plots in Fig. 4. First, steady-state flow, which is indicated by a straight line (constant slope > 0) in these plots, occurs after 10 days of permeation in all cases, except in the case of *W*/*D* = 1 where the flow through the underdrain essentially stopped (slope = 0) after 10 days. Although complete cessation of percolation through the underdrain was not expected on the basis of the previous studies involving numerical simulations [e.g., Chiu and Shackelford (1994) and Shackelford et al. (1994)], the complete cessation of percolation for the case where *W*/*D* = 1 is consistent with some of the results reported in Table 1. Second, the amount of water per unit area that percolates through the foundation layer is greater than the amount of water per unit area that percolates through the sand underdrain regardless of the value for *W*/*D*. Third, after steady-state flow, the slopes of the plots in Fig. 4 for the foundation layer to the left of the sand underdrain are approximately equal to the slopes of the plots for the foundation layer to the right of the sand underdrain for a given *W*/*D* value. Thus, flow at steady state is essentially symmetric with respect to the sand underdrain regardless of the value for *W*/*D*. Finally, the amount of percolated water per unit area through the sand underdrain increases as the value for *W*/*D* increases from 1 to 5 (i.e., as the width, or collection area, of the underdrain increases for a given thickness of the finer soil).

The same general trends apparent in the data shown in Fig. 4 for the tests performed immediately after compaction generally also are apparent in the data shown in Fig. 5 for the tests performed after air drying the soil mixtures for 24 h. In particular, steady-state flow was essentially achieved after 10

days of testing, and the observed lateral flow effect increases as the W/D ratio decreases from 5 to 1. Thus, air drying the soil mixtures for 24 h prior to testing did not result in a significant time lag with respect to the establishment of steady-state flow conditions.

However, a comparison of the results in Figs. 4 and 5 shows that the difference in the normalized cumulative percolation through the sand underdrain for the tests with $W/D = 1$ and $W/D = 2.5$ in Fig. 5 is not as distinct as previously noted in Fig. 4. Also, the data in Fig. 5 for the case where $W/D = 1$ indicate that water continued to percolate through the sand underdrain throughout the duration of the test, an observation that is in stark contrast to the test performed immediately after compaction (Fig. 4). Because air drying the barrier soil mixture increases the initial suction and decreases the hydraulic conductivity of the barrier soil mixture (Fig. 2), the initial contrast in hydraulic conductivity of the barrier layer relative to the sand underdrain may have been lower than when the barrier layer was tested immediately after compaction. This reduction in the contrast in hydraulic conductivity may have been sufficient to allow water to continue to percolate through the sand underdrain during the test for the case where $W/D = 1$.

As shown in Fig. 6, steady-state flow through each area of the testing cell again occurred after approximately 10 days of flow. In addition, the slopes of the plots of normalized cumulative percolation versus time for steady-state conditions are essentially identical for each underdrain in the case of two underdrains as well as for the left and right areas of the foundation layer for all three tests. As a result, the overall flow at steady state was essentially symmetric for each test with respect to the centerline of the testing cell.

Also as shown in Fig. 6 for the case of two underdrains, the total amount of water per unit area that percolates through the foundation layer in the middle of the testing cell is noticeably greater than the total amounts of water per unit area that percolate through the other areas of the testing cell. This observation is consistent with funneling of flow that has been diverted around the underdrains. Also, the reduction in the amount of flow that is funneled through the middle portion for

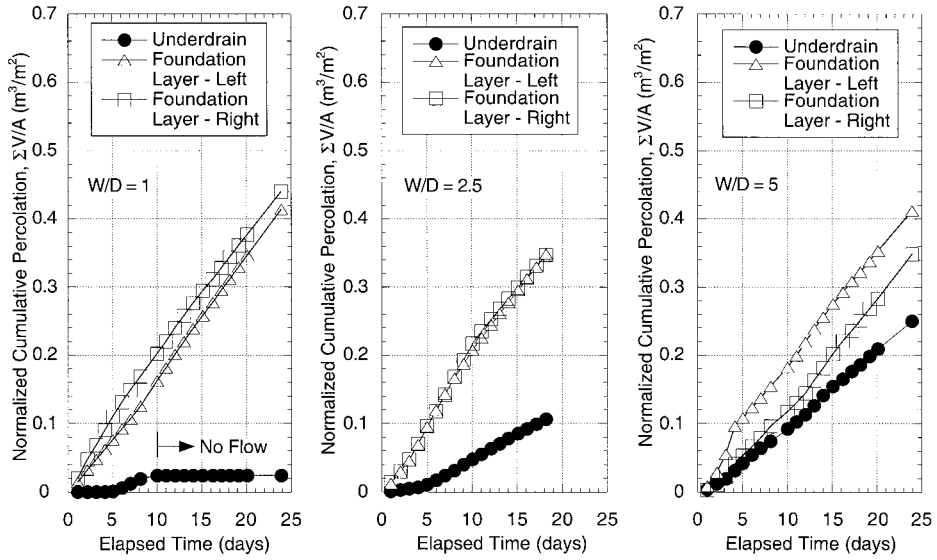

FIG. 4. Normalized Cumulative Percolations for Different Underdrain Size Ratios, *W/D*, for Tests Performed Immediately after Compacting Sand-Kaolin Mixtures

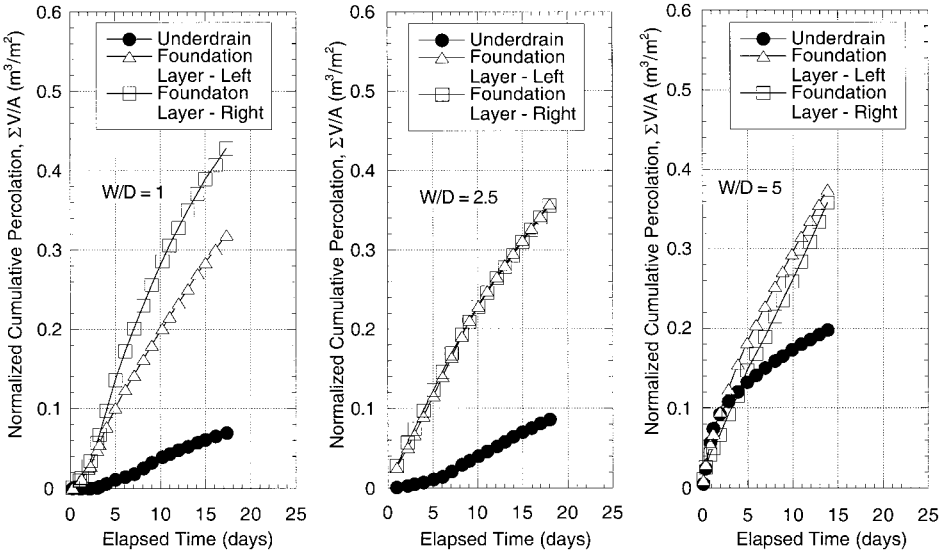

FIG. 5. Normalized Cumulative Percolations for Different Underdrain Size Ratios, *W/D*, for Tests Performed after Air Drying Compacted Sand-Kaolin Mixtures

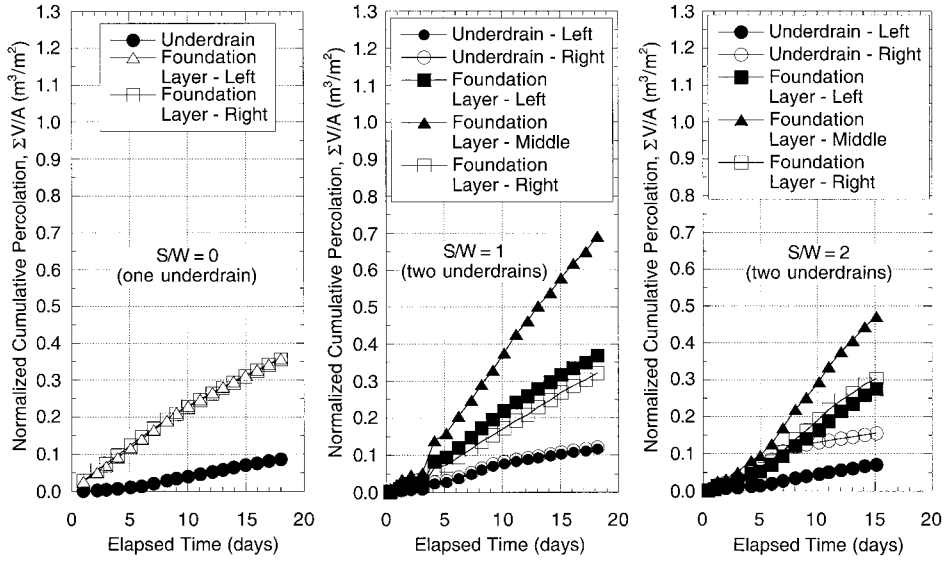

FIG. 6. Normalized Cumulative Percolations for Different Underdrain Spacing Ratios, *S*/*W*, for Tests Performed after Air Drying Compacted Sand-Kaolin Mixtures with *W*/*D* = 2.5

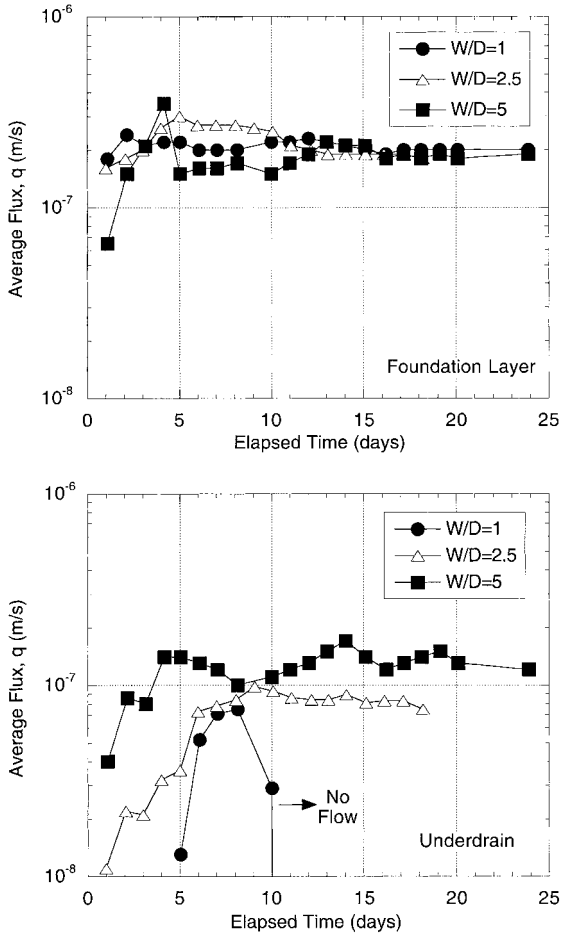

FIG. 7. Average Fluxes through Foundation Layer and Sand Underdrain for Different Underdrain Size Ratios, *W*/*D*, for Tests Performed Immediately after Compacting Sand-Kaolin Mixtures

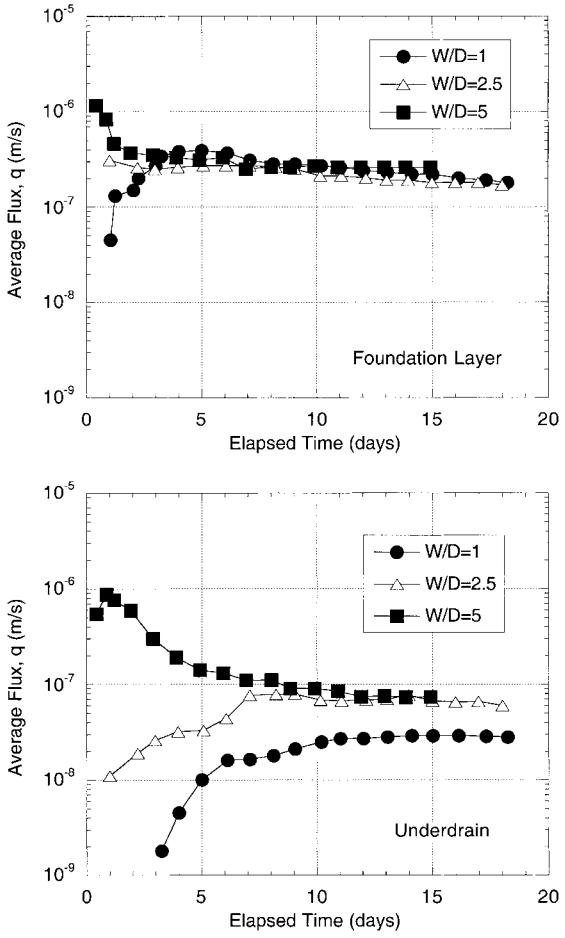

FIG. 8. Average Fluxes through Foundation Layer and Sand Underdrain for Different Underdrain Size Ratios, *W*/*D*, for Tests Performed after Air Drying Compacted Sand-Kaolin Mixtures

S/W = 2 (Test No. 8) relative to S/W = 1 (Test No. 7) for a given elapsed time (e.g., 15 days) is consistent with the greater spacing between the underdrains in the case of S/W = 2.

Average Fluxes

The average fluxes through the foundation layer and the sand underdrain as a function of the underdrain size ratio for the results from tests performed immediately after compaction (Test Nos. 1–3) are shown in Fig. 7. The fluxes reported in Fig. 7 represent the total volumetric flow normalized with respect to the total cross-sectional area of the foundation layer or the sand underdrain divided by the increment in time between measurements. As indicated in Fig. 7, the average fluxes through the foundation layers are close at steady state and

virtually independent of W/D. However, a significant effect of W/D on the average flux through the sand underdrain is apparent, with the average flux decreasing with decreasing value for W/D such that no flux is apparent after 10 days for the test with $W/D = 1$. Thus, the tendency for lateral flow around the underdrain increases as the underdrain collection area becomes smaller relative to the thickness of the barrier layer. This same effect was observed by Chiu and Shackelford (1994) on the basis of numerical simulations of unsaturated flow through similarly layered soil profiles.

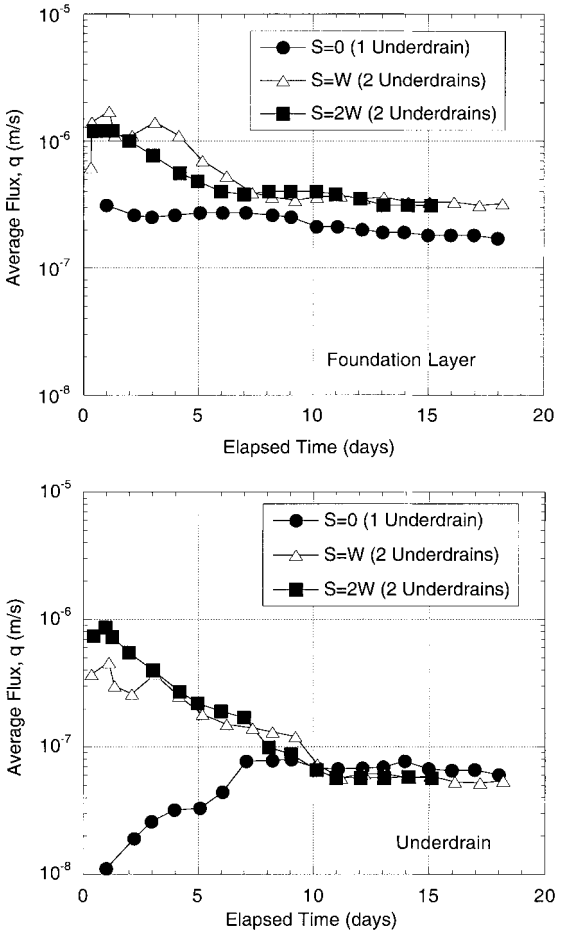

FIG. 9. Average Fluxes through Foundation Layer and Sand Underdrain(s) for Different Underdrain Spacing Ratios, *S*/*W*, for Tests Performed after Air Drying Compacted Sand-Kaolin Mixtures with *W*/*D* = 2.5

The average fluxes through the foundation layer and the sand underdrain as a function of the underdrain size ratio for the results from tests after allowing the soil mixtures to air dry for 24 h (Test Nos. 4–6) are shown in Fig. 8. Similar to the tests performed immediately after compaction, the average fluxes through the foundation layer are close at steady state and virtually independent of W/D. However, the steady-state fluxes through the sand underdrains for $W/D = 2.5$ and $W/D = 5$ are almost the same, and any effect of W/D on the average flux through the sand underdrain is apparent only for the test with $W/D = 1$. Thus, based on the average fluxes through the sand underdrain, the observed lateral flow effect is apparent only for the smallest underdrain size ratio.

The average fluxes through the foundation layer and the sand underdrain(s) as a function of the underdrain spacing for the case where more than one underdrain was used in the test (Test Nos. 7 and 8) are compared in Fig. 9 with the average fluxes for Test No. 5 with the same W/D (=2.5) and only one sand underdrain (i.e., $S/W = 0$). As shown in Fig. 9, the average fluxes through the foundation layers in the case of two underdrains are essentially independent of the underdrain spacing at steady state and also are slightly higher than the average flux through the foundation layer in the case of the single drain. This last observation is expected because two underdrains occupy more space and divert more flow than only one underdrain. However, the average fluxes through the underdrains at steady state are independent not only of the spacing between the two underdrains but also of the number of underdrains.

Hydraulic Conductivity

The hydraulic conductivity of the barrier layer, k_{BL}, was calculated using the same procedure for calculating the in situ hydraulic conductivity of clay liners with underdrains (Daniel 1989). In general, this procedure involves calculating the hydraulic conductivity based on the measured flux into the underdrain in accordance with Darcy's law assuming 1D, saturated flow. Flow through the underdrain also is assumed to be instantaneous (i.e., no water storage), and the suction at the interface between the clay liner (i.e., barrier layer) and the

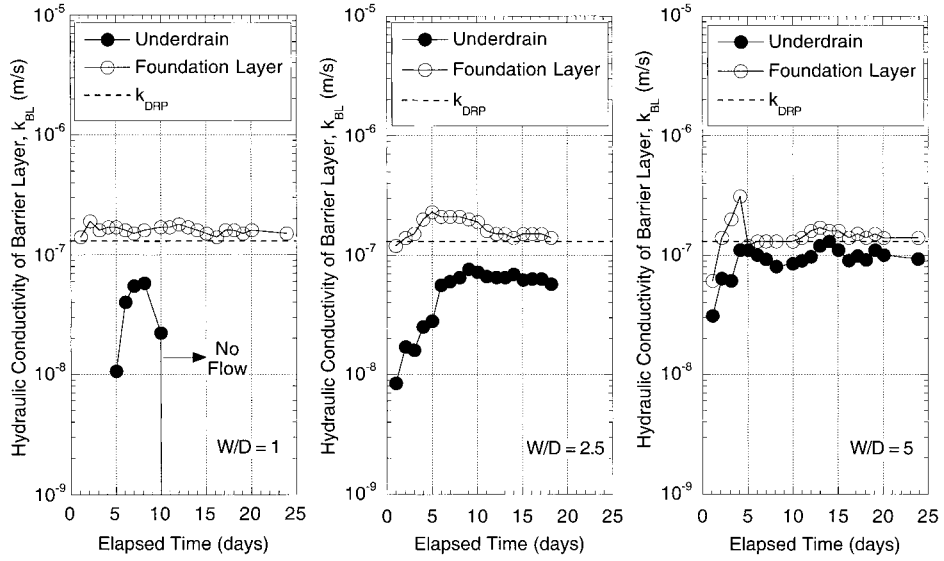

FIG. 10. Hydraulic Conductivity of Barrier Layer Based on Average Flux through Sand Underdrain and Foundation Layer for Different Underdrain Size Ratios, *W*/*D*, for Tests Performed Immediately after Compacting Sand-Kaolin Mixtures [Note: k_{DRP} = Steady-State Hydraulic Conductivity of Barrier Soil Mixture from Chiu and Shackelford (1998)]

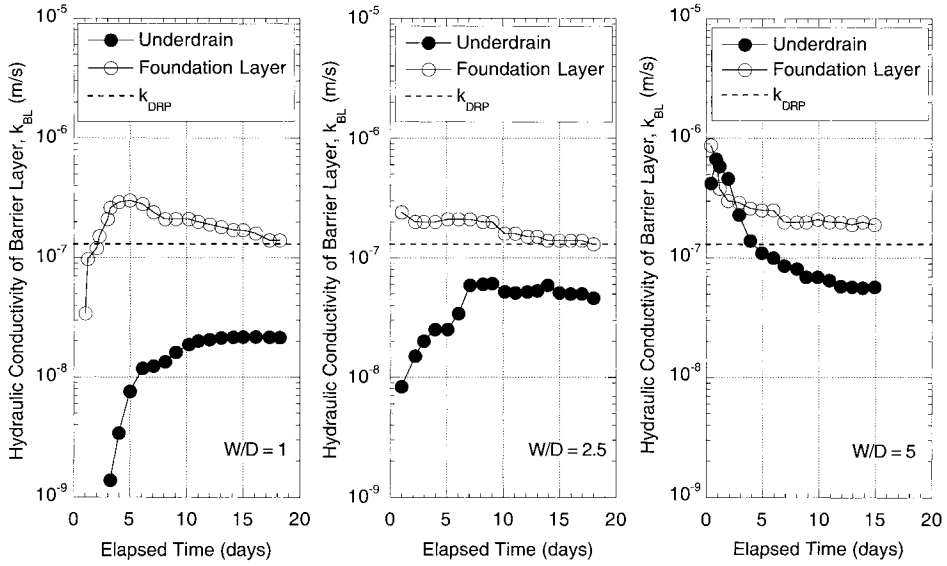

FIG. 11. Hydraulic Conductivity of Barrier Layer Based on Average Flux through Sand Underdrain and Foundation Layer for Different Underdrain Size Ratios, *W/D*, for Tests Performed after Air Drying Compacted Sand-Kaolin Mixtures [Note: k_{DRP} = Steady-State Hydraulic Conductivity of Barrier Soil Mixture from Chiu and Shackelford (1998)]

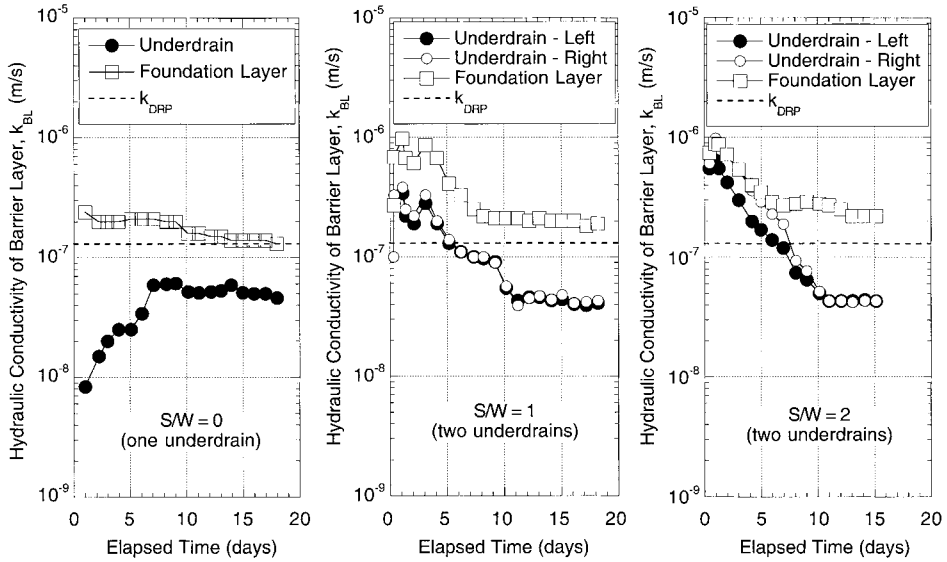

FIG. 12. Hydraulic Conductivity of Barrier Layer Based on Average Flux through Sand Underdrain(s) and Foundation Layer for Different Underdrain Spacing Ratios, *S/W*, for Tests Performed after Air Drying Compacted Sand-Kaolin Mixtures with *W/D* = 2.5 [Note: k_{DRP} = Steady-State Hydraulic Conductivity of Barrier Soil Mixture from Chiu and Shackelford (1998)]

drainage material (i.e., sand underdrain) generally is not measured and, therefore, is assumed to be zero. Therefore, the hydraulic gradient, i, is defined as $(D_p + D)/D$, where D_p is the height of ponded water. In the present study, $D_p = D/3$ such that $i = 1.33$, and $k_{BL} = q/1.33$ (=0.752q), where q represents the average flux through the sand underdrain.

The hydraulic conductivity of the barrier layer also was estimated on the basis of the average flux through the foundation layer. In this case, the assumption that $i = 1.33$ is poorer because the head loss in the foundation layer is not negligible relative to the total head loss. For example, based on the assumption of 1D, saturated flow through the barrier and foundation layers using the k_{DRP} values from Table 3 and assuming equal thicknesses for both layers, the head loss in the foundation layer represents approximately 16% of the total head loss. However, the distribution of total head along the interface between the barrier layer and foundation layer actually varies due to the observed lateral flow effect, with 1D flow conditions being approached only as the distance along the interface from the underdrain increases. Thus, the head loss through the barrier layer also varies with distance along the interface from the underdrain and, therefore, is unknown. As a result, $i = 1.33$ also was assumed in calculating the k_{BL} values based on the average flux through the foundation layer to simplify the analysis, and this approach still provided reasonable estimates of k_{BL} for comparison with the k_{BL} values calculated on the basis of the average flux through the sand underdrain.

The resulting k_{BL} values are plotted versus elapsed time for the case of a single underdrain in Figs. 10 and 11, and for the case of two underdrains in Fig. 12. The independently measured hydraulic conductivity, k_{DRP}, for the barrier soil mixture of 1.3×10^{-7} m/s reported in Table 3 also is shown in each plot for comparison. Although the trends in the calculated k_{BL} for a given W/D (Figs. 10 and 11) or S/W (Fig. 12) vary, the steady-state k_{BL} based on the average flux through the sand underdrain is lower than k_{DRP} for all W/D and S/W values,

whereas the steady-state k_{BL} based on the average flux through the foundation layer generally is closer to the independently measured k_{DRP} value for the barrier soil mixture. Thus, k_{BL} tends to be underestimated using the measured flux from the sand underdrain and the assumptions of saturated, steady-state flow. These observations are consistent with those previously noted by Chiu and Shackelford (1994) and Shackelford et al. (1994) on the basis of numerical simulations.

DISCUSSION

Effect of Underdrain Size

The results reported in this study are in stark contrast to the assumption of saturated, steady-state flow through layered heterogeneous soils that predicts greater flow through the sand underdrain than through the foundation layer due to the higher saturated (maximum) hydraulic conductivity of the sand relative to the coarser soil [e.g., Freeze and Cherry (1979)]. However, all of the results in this study are consistent with Fig. 1 and the contrast in unsaturated soil properties of the sand and sand-kaolin mixtures shown in Fig. 2 as described subsequently.

Although the sand underdrain probably was close to saturation immediately after placement and compaction into the lower portion of the test cell, subsequent gravity drainage before assembling the top and bottom portions of the testing cell probably reduced the initial water content in the sand underdrain relatively rapidly following placement. Thus, the initial volumetric water content of the sand underdrain probably was closer to the field capacity for the sand, which commonly is assumed to occur at a suction of ~33 kPa, or ~3.4 m of water [e.g., Jury et al. (1991)]. Based on the soil-water characteristic data for the sand shown in Fig. 2(a), this suction corresponds to $\Theta \approx 0$ for the sand [i.e., $\theta \approx \theta_r$, see (1)], whereas Θ is closer to the as-compacted values of 0.84 and 0.66 for the barrier soil mixture and foundation soil mixture, respectively, because these soil mixtures do not drain as rapidly as the sand. Thus, the initial suction should be higher in the sand underdrain than in either the barrier layer or the foundation layer [Fig. 2(a)], and, accordingly, the hydraulic conductivity in the sand underdrain should be lower than the hydraulic conductivities of the barrier and foundation layers [Fig. 2(b)]. In this case, at least a portion of the incipient water flux that passes through the barrier layer cannot be transmitted through the sand underdrain resulting in preferred flow around, rather than through, the sand underdrain. Because this same gravity drainage of an initially soaked underdrain also is expected in the field scenario, the observed trends in the data also are expected in the typical field scenario involving use of underdrains to measure the in situ hydraulic conductivity of compacted clay liners.

As shown in Fig. 13 for the ''as-compacted'' tests, the ratio of the steady-state hydraulic conductivity value for the barrier layer, k_{BL}, based on the measured flux from the underdrain to independently measured steady-state hydraulic conductivity for the barrier soil mixture, k_{DRP}, ranges from 0 at $W/D = 1$ to ~0.8 at $W/D = 5$, whereas the ratio of the steady-state k_{BL} value calculated on the basis of the measured flux from the foundation layer to k_{DRP} ranges from ~1.15 at $W/D = 1$ to ~1.0 at $W/D = 5$. The slight increase in k_{BL}/k_{DRP} with a decrease in W/D can be attributed to (1) the increased flux through the foundation layer resulting from the decreased flux through sand underdrain with decreasing W/D; (2) the assumption that $i = 1.33$ as previously discussed; and/or (3) the possibility of slight variations in specimen preparation. Nonetheless, the measured flux from the foundation layer provides reasonably close estimates of k_{DRP} for all three W/D values used in this study.

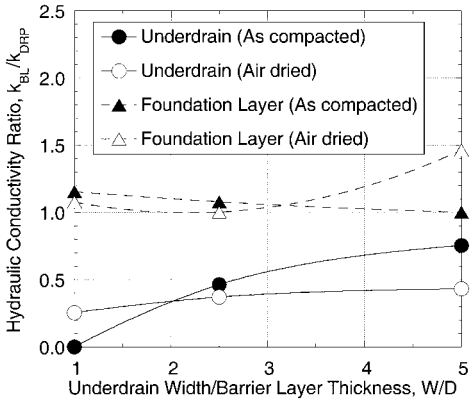

FIG. 13. Effect of Underdrain Size Ratio, *W/D*, on Ratio of Steady-State Hydraulic Conductivity of Barrier Layer, k_{BL}, Based on Average Flux from Sand Underdrain or Foundation Layer to Independently Measured Hydraulic Conductivity of Barrier Soil Mixture, k_{DRP}, for Air-Dried and As-Compacted Initial Conditions [k_{DRP} from Chiu and Shackelford (1998)]

Also, as indicated in Fig. 13, air drying the soils has little effect on the k_{BL} values calculated using the average flux through the foundation layer except for the test where $W/D = 5$. However, there is a noticeable effect of air drying the soils on the k_{BL} values calculated using the average flux through the sand underdrain for all three W/D values. For example, at $W/D = 1$, air drying the soils prior to permeation resulted in a higher steady-state k_{BL} than when the soils were tested immediately after compaction. As previously discussed, the higher measured k_{BL} for the air-dried condition may be attributed, in part, to a reduction in contrast of the hydraulic conductivity between the barrier layer and the sand underdrain (i.e., relative to the as-compacted test) upon air drying resulting in a greater capability of the sand underdrain to transmit the incipient flux from the barrier layer.

Effect of Underdrain Spacing

As in the case for a single underdrain with different underdrain size ratios (W/D), the k_{BL} values based on the average fluxes through the sand underdrains underestimate k_{DRP} and are virtually identical in magnitude at steady state, as shown in Fig. 14. However, the steady-state k_{BL} values based on the average fluxes through the foundation layer are overestimated relative to k_{DRP} when two underdrains are used in the test, a direct consequence of the higher average flux resulting from the funneling of flow through the foundation layer in the case of two underdrains as previously discussed in connection with Fig. 8.

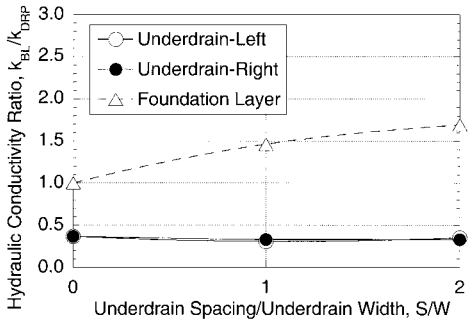

FIG. 14. Effect of Underdrain Spacing Ratio, *S/W*, on Ratio of Steady-State Hydraulic Conductivity of Barrier Layer, k_{BL}, Based on Average Flux from Either Sand Underdrain(s) or Foundation Layer to Independently Measured Hydraulic Conductivity of Barrier Soil Mixture, k_{DRP}, for Tests Performed after Air Drying Compacted Sand-Kaolin Mixtures [k_{DRP} from Chiu and Shackelford (1998)]

Comment on Sidewall Leakage

Sidewall leakage is a potential problem when rigid-wall permeameters are used. However, several observations indicate that sidewall leakage was either negligible or nil in this study and, therefore, was not significant in terms of the test results. First, the normalized percolation rates for each test are essentially symmetric with respect to the test apparatus. Second, the normalized percolation rates, average fluxes, and calculated hydraulic conductivities are consistent among successive tests with respect to the expected effect of the tested variable (i.e., underdrain size ratio and underdrain spacing ratio). Third, the steady-state hydraulic conductivity of the barrier layer, k_{BL}, based on the measured average flux through the foundation layer generally is close to the independently measured value for the barrier soil mixture (i.e., k_{DRP}) reported by Chiu and Shackelford (1998) for tests in which sidewall leakage did not occur. Finally, elevated flux rates, rather than reduced flux rates, would have been expected for the sand underdrain had sidewall leakage been present or significant. Thus, sidewall leakage apparently was not a significant factor in the results of this study.

Practical Implications

The results of the experiments performed in this study show that lateral flow around, rather than through, underdrains placed beneath lower permeability media, such as a barrier layer, can occur. This lateral flow effect is consistent with unsaturated flow behavior previously reported in the literature primarily on the basis of numerical simulations, and results from the contrast in unsaturated flow properties among the barrier layer, surrounding foundation soil, and the underdrain. As a result, the hydraulic conductivity of the barrier layer, k_{BL}, at steady state is underestimated based on the procedure commonly used to calculate k_{BL} assuming 1D, saturated flow.

Although the underestimates in the steady-state k_{BL} values reported in this study are less than an order of magnitude, greater differences between the actual k_{BL} and the measured k_{BL} based on the underdrain flux may occur when the contrast in the properties of the porous media is significantly greater than used in this study, such as in the case where the barrier layer is represented by a compacted clay liner with a saturated hydraulic conductivity $\leq 10^{-9}$ m/s. Also, in the case of a compacted clay liner, the times required to reach steady-state flux can be expected to be considerably longer than found in this study (Daniel 1989). In such cases, a significantly unconservative (low) estimate of the saturated hydraulic conductivity of the compacted clay liner based on the measured underdrain flux may result, particularly if the width (size) of the underdrain is small relative to the thickness. Therefore, although the direct application of the results of the tests performed in this study is limited by the choice of porous media and the scale of the tests, the results have potentially significant ramifications with respect to interpretation of hydraulic conductivity values of compacted clay liners determined in situ using underdrains.

CONCLUSIONS

The results of the tests performed in this study are consistent with previously published results based on numerical simulations for similar soil profiles but different soils in that lateral flow occurs around, rather than through, the sand underdrains. In the case of the previously published numerical simulations, the lateral flow effect resulted from the contrast in the unsaturated soil properties, an effect that is analogous to the capillary barrier effect or wicking effect. As a result of lateral flow, the hydraulic conductivity of the barrier layer, k_{BL}, calculated at steady state using the measured underdrain flux assuming 1D, saturated flow is underestimated relative to the independently measured hydraulic conductivity of the barrier soil mixture (k_{DRP}).

In this study, the underestimate in k_{BL} relative to k_{DRP} for the barrier soil mixture increases as underdrain size ratio, W/D, representing the ratio of the width of the sand underdrain to thickness of the barrier layer, decreases from 5 to 1. For example, the ratio of the steady-state k_{BL} based on the measured flux from the underdrain to the k_{DRP} ranges from 0 (no flow) at $W/D = 1$ to ~ 0.8 at $W/D = 5$ for the tests performed immediately after compacting the soils. Thus, the size of the underdrain affects the estimate of k_{BL} based on the use of underdrains, with more accurate estimates of k_{BL} resulting from the use of larger underdrains. Although the results of this study indicate relatively accurate estimates of k_{BL} can be measured when the width of the underdrain is at least 5 times the thickness of the barrier layer, significantly greater underdrain widths probably are required when the contrast in unsaturated soil properties is greater than used in this study, such as in the use of low-permeability ($\leq 10^{-9}$ m/s), compacted clay liners for waste containment.

The expected delay in the time required to achieve steady-state flow conditions resulting from air drying the soil mixtures prior to testing was not observed. However, air drying the soil mixtures prior to testing apparently enhanced the preference for lateral flow around the sand underdrain for $W/D = 2.5$ and $W/D = 5$ such that the estimates of k_{BL} relative to k_{DRP} were less accurate.

The use of two underdrains separated by a distance of either W or $2W$ did not enhance the accuracy of the estimate of k_{BL} relative to the use of only one underdrain at the same underdrain size ratio, W/D. Thus, the use of two separate, but smaller, underdrains probably is not as beneficial in improving the accuracy of the estimate in k_{BL} as is using a single underdrain with a greater W/D.

ACKNOWLEDGMENTS

Financial support for this work was provided by the U.S. National Science Foundation (NSF), Arlington, Va., under Grant MSS-9257305. The opinions expressed in this paper are solely those of the writers and are not necessarily consistent with the policies or opinions of NSF.

APPENDIX. REFERENCES

Benson, C. H., and Khire, M. V. (1995). ''Earthen covers for arid and semi-arid climates.'' *Landfill closures . . . Environmental protection and landfill recovery, Geotech. Spec. Publ. No. 53*, R. J. Dunn and U. P. Singh, eds., ASCE, New York, 201–217.

Bews, B. E., Barbour, S. L., Wilson, G. W., and O'Kane, M. A. (1997). ''The design of lysimeters for a low flux cover system over acid generating waste rock.'' *Proc., 50th Can. Geotech. Conf. of the Can. Geotech. Soc.*, National Research Council of Canada, Ottawa, 26–33.

Bews, B. E., Wickland, B., and Barbour, S. L. (1999). ''Lysimeter design in theory and practice.'' *Proc., Tailings and Mine Waste '99*, Balkema, Rotterdam, The Netherlands, 13–21.

Bonaparte, R., and Gross, B. A. (1990). ''Field behavior of double-liner systems.'' *Waste containment systems: Construction, regulation, and performance*, R. Bonaparte, ed., ASCE, New York, 52–83.

Cartwright, K., and Krapac, I. G. (1990). ''Construction and performance of a long-term earthen liner experiment.'' *Waste containment systems: Construction, regulation, and performance, Geotech. Spec. Publ. No. 26*, R. Bonaparte, ed., ASCE, New York, 135–156.

Chiu, T.-F. (1995). ''Collection lysimeters for in situ monitoring of compacted clay liners.'' *Proc., Tailings and Mine Waste '95*, Balkema, Rotterdam, The Netherlands, 1–9.

Chiu, T.-F., and Shackelford, C. D. (1994). ''Practical aspects of the capillary barrier effect for landfills.'' *Proc., 17th Int. Madison Waste Conf.*, Dept. of Engrg. Professional Development, University of Wisconsin-Madison, Wis., 357–375.

Chiu, T.-F., and Shackelford, C. D. (1998). ''Unsaturated hydraulic conductivity of compacted sand-kaolin mixtures.'' *J. Geotech. and Geoenvir. Engrg.*, ASCE, Reston, Va., 124(2), 160–170.

Daniel, D. E. (1989). ''In situ hydraulic conductivity tests for compacted clay.'' *J. Geotech. Engrg.*, ASCE, 115(9), 1205–1226.
Freeze, R. A., and Cherry, J. A. (1970. *Groundwater*, Prentice-Hall, Englewood Cliffs, N.J.
Gordon, M. E., Huebner, P. M., and Miazga, T. J. (1989). ''Hydraulic conductivity of three landfill clay liners.'' *J. Geotech. Engrg.*, ASCE, 115(8), 1148–1160.
Jury, W. A., Gardner, W. R, and Gardner, W. H. (1991). *Soil physics*, 5th Ed., Wiley, New York.
Khire, M. V., Benson C. H., and Bosscher, P. J. (1999). ''Field data from a capillary barrier and model predictions with UNSAT-H.'' *J. Geotech. and Geoenvir. Engrg.*, ASCE, 125(6), 518–527.
Kmet, P., and Lindorff, D. E. (1983). ''Use of collection lysimeters in monitoring sanitary landfill performance.'' *Proc., Characterization and Monitoring of the Vadose (Unsaturated) Zone*, National Ground Water Association, Westerville, Ohio, 554–579.
Morel-Seytoux, H. J. (1993). ''Dynamic perspective on the capillary barrier effect at the interface of an upper fine layer with a lower coarse layer.'' *Proc., Symp. on Engrg. Hydro.*, C. Y. Kuo, ed., ASCE, New York, 467–472.
Morris, C. E., and Stormont, J. C. (1997). ''Capillary barriers and subtitle D covers: Estimating equivalency.'' *J. Envir. Engrg.*, ASCE, 123(1), 3–10.
Reades, D. W., Lahti, L. R., Quigley, R. M., and Bacopoulos, A. (1990). ''Detailed case history of clay liner performance.'' *Waste containment systems: Construction, regulation, and performance, Geotech. Spec. Publ. No. 26*, R. Bonaparte, ed., ASCE, New York, 156–174.
Reades, D. W., Poland, R. J., and Kelly, G. (1987). ''Discussion of 'Hydraulic conductivity of two prototype clay liners,' by Steven R. Day and David E. Daniel.'' *J. Geotech. Engrg.*, ASCE, 113(7), 809–813.
Sai, J. O., and Anderson, D. C. (1990). ''Field hydraulic conductivity tests for compacted soil liners.'' *Geotech. Testing J.*, 13(3), 215–225.
Sailie, L. (1985). ''Some aspects of sandwiched soil cover design for toxic waste repositories.'' *Engrg. Geol.*, Amsterdam, 21, 321–326.
Shackelford, C. D., Chang, C.-K., and Chiu, T.-F. (1994). ''The capillary barrier effect in unsaturated flow through soil barriers.'' *Proc., 1st Int. Congr. on Envir. Geotechnics*, Bi-Tech Publishing, Richmond, B.C., Canada, 789–793.
Shackelford, C. D., and Chiu, T.-F. (1997). ''The influence of the capillary barrier effect on the use of sand underdrains in waste disposal practice.'' *Geoenvironmental engineering, contaminated ground: Fate of pollutants and remediation*, R. N. Yong and H. R. Thomas, eds., Thomas Telford, London, 357–364.
van Genuchten, M. T. (1980). ''A closed-form equation for predicting the hydraulic conductivity of unsaturated soils.'' *Soil Sci. Soc. Am. J.*, 44(5), 892–898.
Yeh, T.-C., Guzman, A., Srivastava, R., and Gagnard, P. E. (1994). ''Numerical simulation of the wicking effect in liner systems.'' *Ground Water*, 32(1), 2–11.